J. Soil Groundw. Environ. Vol. 21(2), p. 8~14, 2016
http://dx.doi.org/10.7857/JSGE.2016.21.2.008
ISSN 1598-6438 (Print), ISSN 2287-8831 (Online)

≪ Research Paper ≫

Quantitative Comparison of the Photocatalytic Efficiency of TiO_2 Nanotube Film and TiO_2 Powder

Jun-Won Jang[1] · Sung Jik Park[2] · Jae-Woo Park[2]*

[1]*Convergence R&D Team, Pohang Institute of Metal Industry Advancement*
[2]*Department of Civil and Environmental Engineering, Hanyang University*

ABSTRACT

We compared the plausible reaction mechanism and quantitative efficiency of highly self-organized TiO_2 nanotube ($ntTiO_2$) film with TiO_2 powder. Film was fabricated by electrochemical potentiostatic anodization of titanium thin film in an ethylene-glycol electrolyte solution containing 0.3 wt% NH_4F and 2 vol% deionized water. Nanotubes with a pore size of 80-100 nm were formed by anodization at 60 V for 3 h. Humic acid (HA) was degraded through photocatalytic degradation using the $ntTiO_2$ film. Pseudo first-order rate constants for 0.3 g of $ntTiO_2$, 0.3 g TiO_2 powder, and 1 g TiO_2 powder were 0.081 min^{-1}, 0.003 min^{-1}, and 0.044 min^{-1}, respectively. HA adsorption on the $ntTiO_2$ film was minimal while adsorption on the TiO_2 powder was about 20% based on thermogravimetric analysis. Approximately five-fold more normalized OH radicals were generated by the $ntTiO_2$ film than the TiO_2 powder. These quantitative findings explain why $ntTiO_2$ film showed superior photocatalytic performance to TiO_2 powder.

Key words : TiO_2 nanotubes, Electrostatic anodization, Humic acid, Adsorption effect, Terephthalic acid

1. Introduction

Semiconducting catalysts can be used to mineralize organic contaminants, such as aromatics, halohydrocarbons, HA and so on, in natural groundwater (Haga and Yosomiya, 1997, Wold, 1993). Titanium dioxide (TiO_2), especially in anatase form, is one of the most significant catalysts in environmental applications (Fujishima et al., 2000, Fujishima and Zhang, 2006, Kim et al., 2014). It has been applied mostly in the form of glass or glass fibers, but more practical forms of this semiconductor photocatalyst are in films or on ceramic substrates (Choi, 2006, Jang and Park, 2011). A sol-gel process with heat treatment of titanium sol material is most commonly utilized to produce TiO_2 in film form (Carotta et al., 2007, Haga et al., 1997, Quan et al., 2009). Aerosol pyrolysis and hydrolysis with different alkoxides or titanium-containing compounds are also used (Aromaa et al., 2007, Luyo et al., 2007, Subba Ramaiah and Sundara Raja, 2006). It is, however, difficult to produce pure TiO_2 film because of residual impurities. Crystal defects in TiO_2 due to these impurities are the cause of reduced catalytic activity. Porous oxide growth in alumina has motivated electrochemical synthesis of oxide nanostructures with various metals (Jang et al., 2009, Karlinsey, 2005, Lee and Smyrl, 2005, Mukherjee et al., 2003, Tsuchiya and Schmuki, 2005). Certain metal oxide nanostructures possess dramatically improved charge transport properties, enabling a variety of advanced applications. Self-organized TiO_2 nanotube ($ntTiO_2$) film has received considerable attention in recent years because it shows remarkable performance in a variety of applications. This is due to the high surface area, stability, and excellent charge transfer properties of this type of film (Liu et al., 2008, Mor et al., 2006, Nischk et al., 2014, Yang et al., 2006, Yun et al., 2013, Zhang et al., 2007).

Our objective in this research was to quantitatively compare the photocatalytic efficiencies of $ntTiO_2$ thin film and TiO_2 powder. Although $ntTiO_2$ film has been suggested as a replacement for TiO_2 powder, the photocatalytic activity of $ntTiO_2$ film versus TiO_2 powder has not been compared

*Corresponding author : jaewoopark@hanyang.ac.kr
Received : 2015. 12. 7 Reviewed : 2015. 12. 16 Accepted : 2015. 12. 23
Discussion until : 2016. 6. 30

directly. $ntTiO_2$ thin film evaluated in this research was produced by electrostatic anodization. Photoreactivity of the $ntTiO_2$ film was demonstrated by measuring OH radical formation rate under UV irradiation. $ntTiO_2$ films were characterized by Field-emission scanning election microscopy (FE-SEM), X-ray diffraction (XRD), and energy-dispersive X-ray (EDX) spectroscopy.

2. Material and Methods

2.1. Fabrication of $ntTiO_2$ film via electrostatic anodization

Titanium (Ti) film (99.5% pure and 25 μm thick) was purchased from Alfa Aesar and was cut into 20 mm × 60 mm sections. Ti film was then placed in a mixture of HF, HNO_3, and H_2O at a volume ratio of 1:4:5 for 30 to 60 sec to remove impurities on the surface. This was followed by chemical etching, washing with deionized water for 20 min, and drying for anodization. Ethylene glycol (EG) electrolyte solution containing 0.3 wt% NH_4F and 2 vol% deionized water was used. TiO_2 array films were synthesized by electrostatic anodization of titanium foil as an anode in a two-electrode system (Paulose et al., 2007). Platinum (99.9% pure) was used as cathode. Distance between the two poles was fixed at 5 cm. Anodization was performed at a constant voltage of 60 V for 3 h using a regulated DC power supply with a maximum current of 5 A and maximum voltage of 160 V (EP1605, PNCYS). Temperature of the electrolyte solution was adjusted to 15ºC using coolant. The thin-film sample was stored in a vacuum desiccator after surface cleaning with distilled water. Heat treatment was carried out in electric furnace at 400-450ºC to convert the TiO_2 into anatase form, which is the most photoactive among the three TiO_2 crystal forms of brookite, anatase, and rutile. All chemical reagents were from Aldrich.

2.2. Photocatalysis

Humic acid (HA) was the target contaminant in this research as it is a precursor of trihalomethanes (Li et al., 2002, Yang and Lee, 2006). HA used was technical grade from Aldrich. Batch experiments to confirm the photocatalytic activity of the produced $ntTiO_2$ were performed in a circular reactor with a 500 mL reactor column made with quartz, a Sankyo 16 W (UV-C) UV lamp, a magnetic stirrer, and a pump. The concentration of stock HA solution was 1,000 mg/L and it was diluted to 10 mg/L for batch experiments. Anatase-phase TiO_2 powder (Showa) was put into HA solution for photocatalytic degradation experiments for comparison with the powder form. At different time intervals, 3-mL aliquots of HA solution were collected and analyzed.

2.3. Characterization and analysis

Surface morphologies of the samples were observed using a scanning electron microscope (SEM) with an acceleration voltage of 15.0 kV (JEOL, JJSM-6340F). Changes in crystal structure before and after calcination treatment were monitored with an X-ray diffractometer (XRD) using 1.5406 Å of CuKα radiation (λ) from 20° to 80° at a scanning speed of $5°min^{-1}$ (RIGAKU, D/MAX-2500/PC). An energy-dispersive X-ray (EDX) spectrophotometer was used for elemental analysis of the surface. HA concentration was analyzed using a total organic carbon (TOC) analyzer (Analytic Jena, Multi N/C 3100). Adsorption mass measurement with external light blocked out was done with a thermogravimetric analyzer (Perkin Elmer, TGA7) under N_2 from 30ºC to 700ºC at a rate of increase of 5ºC/min. Fluorescence spectra and OH radicals were measured using a fluorescence spectrophotometer (Scinco, FluoroMate FS-2) excited by a 150 W Xe lamp. Terephthalic acid (TA) was used as a fluorescence probe because it can react with OH radicals in basic solution to generate 2-hydroxy TA (TAOH), which emits a unique fluorescence signal with a spectrum peak around 426 nm (Hirakawa and Nosaka, 2002, Yang et al., 2009). Most TiO_2 particles were precipitated by adding KCl, after which light scattering became negligible. Because TAOH molecules were not adsorbed on the TiO_2 powder and $ntTiO_2$ in the presence of KCl at pH 11.5, all TAOH produced was assumed to be in the supernatant. The mass of TAOH produced was determined by fluorescence intensity.

3. Results and Discussion

3.1. Characterization

Fig. 1 shows the surface morphology of $ntTiO_2$ produced by electrostatic anodization. Nanotubes with a pore size of

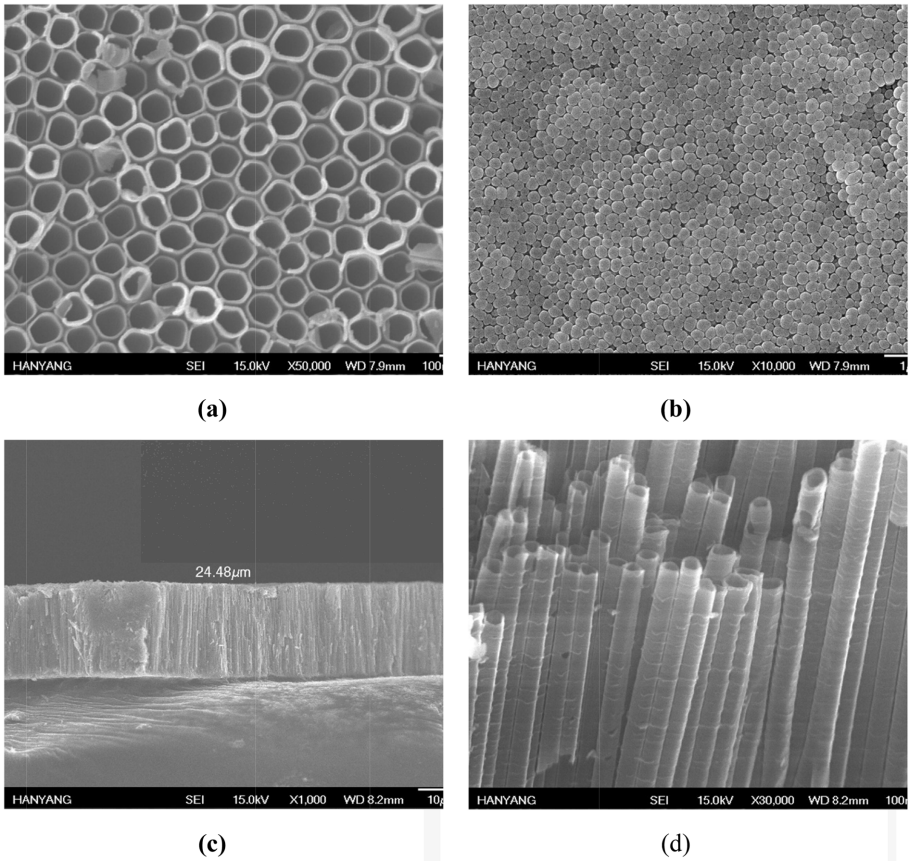

Fig. 1. FE-SEM image of the $ntTiO_2$ film in this research via electrostatic anodization: (a) top, (b) bottom, (c) cross-section, and (d) side.

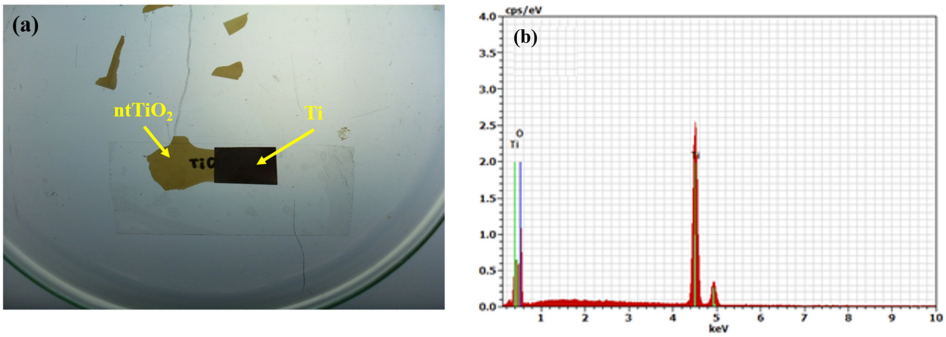

Fig. 2. (a) A transparent $ntTiO_2$ film and (b) its chemical composition.

80-100 nm formed after anodization at 60 V for 3 h. Nanotubes were about 25 μm-long at both 20 V and 40 V, consistent with a previous study that showed that nanotube growth rate is proportional to anodization time rather than voltage.

Fig. 2(a) shows $ntTiO_2$ exposed to visible light. Handwritten letters, "Ti", were clearly visible at the $ntTiO_2$ part while the letters, including part of "O", under $ntTiO_2$/Ti could not be readily seen. The body of $ntTiO_2$ was physically very weak; a support was therefore required for the film form and thermal treatment was used to enhance the structural strength of $ntTiO_2$. $ntTiO_2$ on Ti films was used after electrostatic anodization. Results of EDX analysis of the $ntTiO_2$/Ti pattern of TiO_2 are shown in Fig. 2(b). The chemical composition of $ntTiO_2$ was 69% Ti, 18% O, and 3.12% C, similar to typical TiO_2.

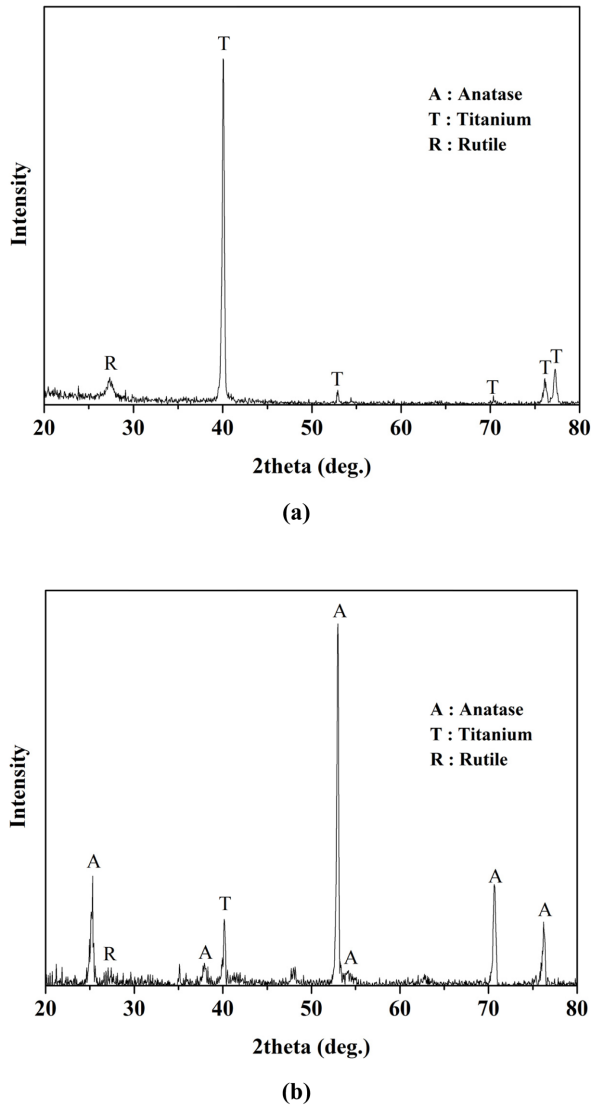

Fig. 3. XRD patterns of thin film: (a) after anodization and (b) with annealing treatment at 450°C for 2 hours at heating and cooling rate of 30°C/min.

Fig. 3(a) shows the XRD pattern of $ntTiO_2$ immediately after anodization and (b) the crystal structure of the film surface after annealing. $ntTiO_2$ film after annealing treatment could assume one of three different forms: brookite, anatase, or rutile. Rutile is stable across a broad range of temperatures, while the other two phases are semi-stable thermodynamically. In particular, brookite is created at high temperatures and pressures. It is very unstable and it is difficult to obtain pure crystals. Anatase crystal was found on non-crystal TiO_2 film with some rutile characteristics after heat treatment at 450°C.

3.2. Theoretical calculation of generated $ntTiO_2$

Diameters and lengths of the $ntTiO_2$ film ranged from 80-100 nm and 2,500 nm, respectively, based on top (Fig. 1(a)) and cross-sectional (Fig. 1(c)) images. The mass of $ntTiO_2$ was measured indirectly using Faraday's law (Jang and Park, 2014):

$$Q = \frac{At}{S} \tag{1}$$

$$L = \frac{QM}{Fn\delta} \tag{2}$$

$$L\delta S = \frac{AtM}{nF} \tag{3}$$

where Q is the circulated charge ($C \cdot cm^{-2}$), A is the electric current, S is the surface area of Ti film, t is the anodization time, M is the molecular weight of the oxide (79.866 g mol^{-1}), F is the Faraday constant (96,487 $C \cdot equiv^{-1}$), n is the number of electrons involved in the reaction, δ is the density of TiO_2 (3.8-4.1 $g \cdot cm^{-3}$), and L is the theoretical length of the nanotube layers. This theoretical mass ($L\delta S$) can be calculated as shown in Eq. (3) using Eqs (1) and (2). The theoretically-calculated mass of the nanotube layers in this research was about 0.102 g per film.

3.3. HA degradation

Photocatalytic experiments to degrade HA in solution were carried out using 0.3 g commercial TiO_2 powder and $ntTiO_2$ film prepared by anodization and annealing at 450°C. Kinetics of HA degradation were fitted with a pseudo-first order rate equation as follows:

$$\frac{C}{C_0} = e^{-k_{obs}t} \tag{4}$$

where C and C_0 are the residual and initial HA concentration (mg/L), respectively. The pseudo-first order rate constant is k_{obs} (min^{-1}). A control experiment without any catalyst was performed with 10 mg/L HA solution; less than 2% of total HA was lost under UV illumination for 90 min. A photolysis test of HA was also performed without catalysis and a light source. Typical thermogravimetric (TGA) curves of photocatalytic samples before and after HA adsorption are presented in Fig. 4. The weight change before and after HA adsorption was about 15% and 2% for 0.3 g of TiO_2 powder and $ntTiO_2$, respectively. Therefore, HA

Table 1. Pseudo first-order rate constants (k, min^{-1}) for HA degradation on various TiO_2

	Catalyst weight (g)		
	0.1	0.3	1
TiO_2 powder	0.001 min^{-1}	0.003 min^{-1}	0.074 min^{-1}
$ntTiO_2$ (theoretical mass)	0.019 min^{-1}	0.081 min^{-1}	–

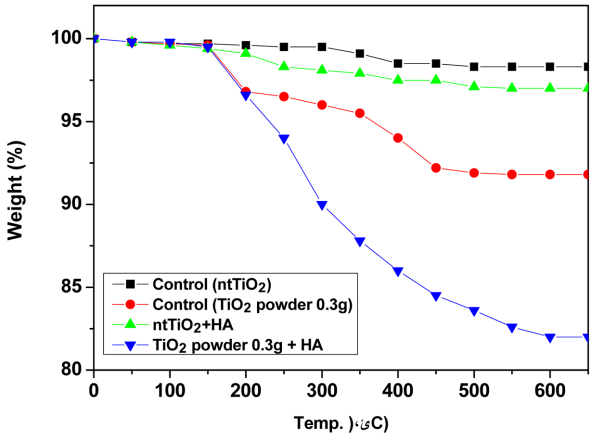

Fig. 4. TGA results from the $ntTiO_2$ and TiO_2 powder form (control: without HA adsorption).

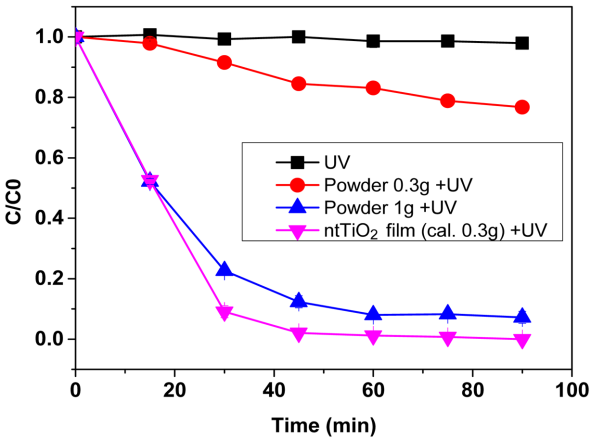

Fig. 5. Photocatalytic degradation of HA using TiO_2 powder form and $ntTiO_2$ film.

removal by adsorption on the $ntTiO_2$ surface was negligible in HA photocatalytic degradation. In addition, aqueous TOC was measured to quantify the HA concentration; degraded HA in this research corresponded to completely-degraded HA.

Two different samples of TiO_2 powder, 0.3 g and 1 g, were evaluated to make a catalytic comparison between $ntTiO_2$ film and TiO_2 powder (see Fig. 5). $ntTiO_2$ film exhibited superior photocatalytic efficiency to TiO_2 powder. HA degradation by $ntTiO_2$ containing a theoretical mass of 0.3 g

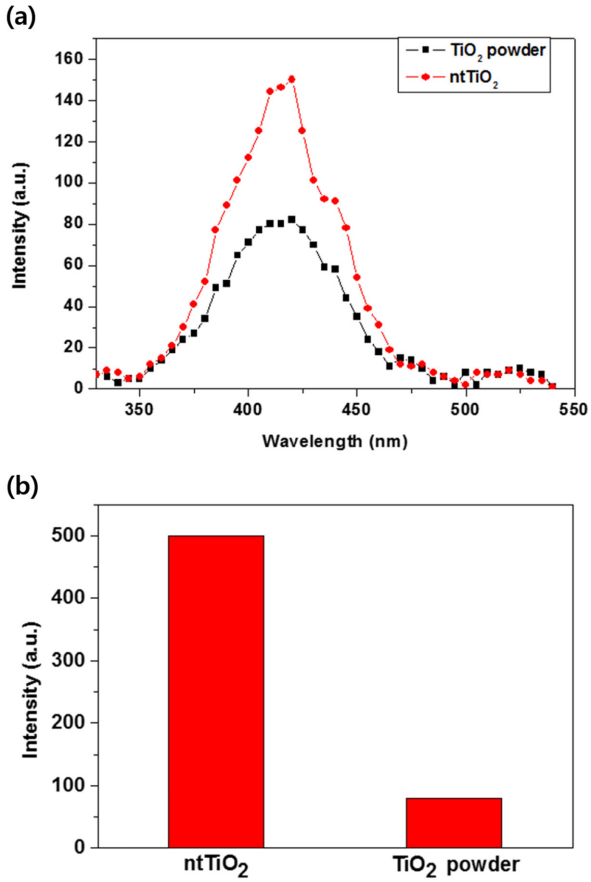

Fig. 6. Fluorescence spectra (a) and normalized fluorescence intensity per unit mass (b) of $ntTiO_2$ and TiO_2 powder form.

TiO_2 was completely finished in 60 min, but HA still remained after 90 min when the TiO_2 powder sample was used. Table 1 showed the pseudo-first order rate constants for HA degradation in photocatalytic reactor systems with TiO_2 powder or $ntTiO_2$ film as photocatalyst.

3.4. Comparison of generated OH radicals

Formation of active hydroxyl radicals upon UV irradiation was monitored. OH radicals react with TA and generate TAOH, which emits fluorescence. As shown in Fig. 6(a), significant fluorescence spectra due to TAOH were generated upon irradiation with 300-600 nm light. The

capability of forming OH radicals per unit mass of $ntTiO_2$ or TiO_2 powder was evaluated. About five-fold more OH radicals were generated from $ntTiO_2$ than TiO_2 powder, as shown in Fig. 6(b). The higher normalized production of OH radicals from $ntTiO_2$ films than TiO_2 powder indicates that $ntTiO_2$ film has superior catalytic efficiency to TiO_2 powder.

$NtTiO_2$ exhibited much lower HA adsorption on its surface than TiO_2 powder, which implies that photogenerated OH radicals were greatly inhibited in $ntTiO_2$. Photogenerated OH radicals of excited $ntTiO_2$ were degraded instantly or blocked HA adsorption from the surface of $ntTiO_2$, resulting in higher photocatalytic activity than the TiO_2 powder. Due to lower HA adsorption on the surface, the photocatalytic effect of the $ntTiO_2$ film was better than that of TiO_2 powder.

4. Conclusions

$NtTiO_2$ film was produced by electrostatic anodization at 60 V in an EG electrolyte solution containing 0.3 wt% NH_4F and 2 vol% deionized water. Anatase phase photocatalytic crystals were formed after annealing treatment at 450ºC. $ntTiO_2$ film containing 0.3 g of theoretical $ntTiO_2$ mass exhibited better photocatalytic performance than 0.3 g and 1 g of TiO_2 powder with respect to HA degradation. HA adsorption on $ntTiO_2$ film was negligible, while adsorption on TiO_2 powder was about 20% based on TGA. Normalized concentration of OH radicals, measured by TAOH fluorescence, was about five times higher for $ntTiO_2$ film than TiO_2 powder. Greater generation of OH radicals by irradiation of the $ntTiO_2$ film than the powder decreased HA adsorption by the film relative to the powder.

Acknowledgements

This study was supported by the Basic Science Research Program through the National Research Foundation of Korea (NRF) funded by the Ministry of Science, ICT, & Future Planning (No. 015R1A2A1A09005838).

References

Aromaa, M., Keskinen, H., Mäkelä and J.M., 2007, The effect of process parameters on the liquid flame spray generated titania nanoparticles, *Biomol. Eng.,* **24**, 543-548.

Carotta, M.C., Gherardi, S., Malagù, C., Nagliati, M., Vendemiati, B., Martinelli, G., Sacerdoti, M., and Lesci, I.G., 2007, Comparison between titania thick films obtained through sol-gel and hydrothermal synthetic processes, *Thin Solid Films*, **515**, 8339-8344.

Choi, W., 2006, Pure and modified TiO_2 photocatalysts and their environmental applications, *Catal. Surv. Asia*, **10**, 16-28.

Fujishima, A., Rao, T.N., and Tryk, D.A., 2000, Titanium dioxide photocatalysis, *J. Photochem. Photobiol. C-Photochem. Rev.*, **1**, 1-21.

Fujishima, A. and Zhang, X., 2006, Titanium dioxide photocatalysis: present situation and future approaches, *C. R. Chim.*, **9**, 750-760.

Haga, Y., An, H., and Yosomiya, R., 1997, Photoconductive properties of TiO_2 films prepared by the sol-gel method and its application, *J. Mater. Sci.*, **32**, 3183-3188.

Hirakawa, T. and Nosaka, Y., 2002, Properties of O_2- and OH formed in TiO_2 aqueous suspensions by photocatalytic reaction and the influence of H_2O_2 and some ions, *Langmuir*, **18**, 3247-3254.

Jang, J.W. and Park, J.W., 2011, Photocatalytic performance of TiO_2 films produced with combination of oxygen-plasma and rapid thermal annealing, *Thin Solid Films*, **520**, 193-198.

Jang, J.W. and Park, J.W., 2014, Iron oxide nanotube layer fabricated with electrostatic anodization for heterogeneous Fenton like reaction, *J. Hazard. Mater.*, **273**, 1-6.

Jang, J.W., Jun, J.E., and Park, J.W., 2009, Fabrication of zero valent iron (ZVI) nanotube film via potentiostatic anodization and electroreduction, *Water Sci. Technol.*, **59**, 2503-2507.

Karlinsey, R.L., 2005, Preparation of self-organized niobium oxide microstructures via potentiostatic anodization, *Electrochem. Commun.*, **7**, 1190-1194.

Kim, L.J., Jang, J.W., and Park, J.W., 2014, Nano TiO_2-functionalized magnetic-cored dendrimer as a photocatalyst, *Appl. Catal. B-Environ.*, **147**, 973-979.

Lee, W.J. and Smyrl, W.H., 2005, Zirconium oxide nanotubes synthesized via direct electrochemical anodization, *Electrochem. Solid State Lett*, **8**, B7-B9.

Li, X.Z., Li, F.B., Fan, C.M., and Sun, Y.P., 2002, Photoelectrocatalytic degradation of humic acid in aqueous solution using a Ti/TiO_2 mesh photoelectrode, *Water Res.*, **36**, 2215-2224.

Liu, Z., Zhang, X., Nishimoto, S., Jin, M., Tryk, D.A., Murakami, T., and Fujishima, A., 2008, Highly ordered TiO_2 nanotube arrays with controllable length for photoelectrocatalytic degradation of phenol, *J. Phys. Chem. C*, **112**, 253-259.

Luyo, C., Fábregas, I., Reyes, L., Solís, J.L., Rodríguez, J., Estrada, W., and Candal, R.J., 2007, SnO_2 thin-films prepared by a spray-gel pyrolysis: Influence of sol properties on film morphologies, *Thin Solid Films*, **516**, 25-33.

Mor, G.K., Varghese, O.K., Paulose, M., Shankar, K., and Grimes, C.A., 2006, A review on highly ordered, vertically oriented TiO_2 nanotube arrays: fabrication, material properties, and solar energy applications, *Sol. Energy Mater. Sol. Cells*, **90**, 2011-2075.

Mukherjee, N., Paulose, M., Varghese, O.K., Mor, G.K., and Grimes, C.A., 2003, Fabrication of nanoporous tungsten oxide by galvanostatic anodization, *J. Mater. Res.*, **18**, 2296-2299.

Nischk, M., Mazierski, P., Gazda, M., and Zaleska, A., 2014, Ordered TiO_2 nanotubes: The effect of preparation parameters on the photocatalytic activity in air purification process, *Appl. Catal. B-Environ.*, **144**, 674-685.

Paulose, M., Prakasam, H.E., Varghese, O.K., Peng, L., Popat, K.C., Mor, G.K., Desai, T.A., and Grimes, C.A., 2007, TiO_2 nanotube arrays of 1000 μm length by anodization of titanium foil: phenol red diffusion, *J. Phys. Chem. C*, **111**, 14992-14997.

Quan, X., Zhao, Q., Tan, H., Sang, X., Wang, F., and Dai, Y., 2009, Comparative study of lanthanide oxide doped titanium dioxide photocatalysts prepared by coprecipitation and sol-gel process, *Mater. Chem. Phys.*, **114**, 90-98.

Subba Ramaiah, K., and Sundara Raja, V., 2006, Structural and electrical properties of fluorine doped tin oxide films prepared by spray-pyrolysis technique, *Appl. Surf. Sci.*, **253**, 1451-1458.

Tsuchiya, H. and Schmuki, P., 2005, Self-organized high aspect ratio porous hafnium oxide prepared by electrochemical anodization, *Electrochem. Commun.*, **7**, 49-52.

Wold, A., 1993, Photocatalytic properties of titanium dioxide (TiO_2), *Chem. Mat.*, **5**, 280-283.

Yang, H.G., Liu, G., Qiao, S.Z., Sun, C.H., Jin, Y.G., Smith, S.C., Zou, J., Cheng, H.M., and Lu, G.Q., 2009, Solvothermal synthesis and photoreactivity of anatase TiO_2 nanosheets with dominant {001} facets, *J. Am. Chem. Soc.*, **131**, 4078-4083.

Yang, J.K. and Lee, S.M., 2006. Removal of Cr(VI) and humic acid by using TiO_2 photocatalysis, *Chemosphere*, **63**, 1677-1684.

Yang, S., Liu, Y., and Sun, C., 2006, Preparation of anatase TiO_2/Ti nanotube-like electrodes and their high photoelectrocatalytic activity for the degradation of PCP in aqueous solution, *Appl. Catal. A-Gen.*, **301**, 284-291.

Yun, D.M., Cho, H.H., Jang, J.W., and Park, J.-W., 2013, Nano zero-valent iron impregnated on titanium dioxide nanotube array film for both oxidation and reduction of methyl orange, *Water Res.*, **47**, 1858-1866.

Zhang, Z., Yuan, Shi, G., Fang, Y., Liang, L., Ding, H., and Jin, L., 2007, Photoelectrocatalytic activity of highly ordered TiO_2 nanotube arrays electrode for azo dye degradation, *Environ. Sci. Technol.*, **41**, 6259-6263.